Korean J. Chem. Eng., **29**(12), 1776-1781 (2012)
DOI: 10.1007/s11814-012-0090-4

Synthesis and characterization of nanocomposite MCM-48-PEHA-DEA and its application as CO_2 adsorbent

Mansoor Anbia†, Vahid Hoseini, and Sakineh Mandegarzad

Research Laboratory of Nanoporous Materials, Faculty of Chemistry, Iran University of Science and Technology, Farjam Street, Narmak, Tehran 16846, Iran
(*Received 18 November 2011 • accepted 7 June 2012*)

Abstract−Three nanocomposites containing MCM-48-35PEHA-15DEA (35 and 15 as weight percent of amine addition), MCM-48-30PEHA-20DEA and MCM-48-25PEHA-25DEA of mesoporous silica MCM-48 modified by the mixture of pentaethylenehexamine (PEHA) and diethanolamine (DEA) have been synthesized and used to study the adsorption of carbon dioxide (CO_2). They are characterized by low angle x-ray diffraction (XRD), Fourier transform infrared (FT-IR) and Brunauer-Emmet-Teller (BET) analysis. MCM-48-35PEHA-15DEA (as optimized adsorbent) shows CO_2 adsorption capacity of 0.51 (m·mol CO_2/g-adsorbent) at 1 bar and 298 K, much higher than CO_2 adsorption capacity on polyethyleneimine, pyrrolidinepropyl and polymerized aminopropyl loaded MCM-48.

Key words: CO_2 Adsorption, Nanocomposite, MCM-48, Amine Modified

INTRODUCTION

Carbon dioxide (CO_2) is usually produced by alcoholic fermentation, coke combustion and other fossil fuels containing carbon [1,2]. Therefore, the separation of this gas and its density preservation according to world standard is important. There are several techniques for capturing CO_2, including physical absorption, chemical absorption, physical adsorption, and membrane separation [3-9].

Adsorbents for removal of CO_2 can be classified into two groups: physisorbents and chemisorbents [10]. Physisorbents such as molecular sieves, activated carbon [11] and zeolites [12] adsorb CO_2 on their surface. Their selectivity towards CO_2 in the presence of other gases (N_2, H_2O, etc.) is still low. The chemisorbents eliminate CO_2 by chemical reaction with this gas. Most of them are amine functionalized supported materials [10]. CO_2 separation with liquid amines by Chemical absorption is widely used in gas and petro-chemical industries. The alkanolamines, such as monoethanolamine, diethanolamine, methyldiethanolamine, and triethanolamine are the most common solvents. These amine-based chemical solvents interact specifically with CO_2 and absorb it selectively [13-15].

Mesoporous silica materials have many applications [16-20]. To increase CO_2 adsorption capacity, basic sites are attached into pore channels of mesoporous silica materials. Shen et al. [21] have reported CO_2 adsorption on La_2O_3-modified MCM-41, Macario et al. [22] have used Al, Fe, Cu and Zn-containing mesoporous materials (MCM-41 and MCM-48). The amino-functional groups were also examined. Chaffee et al. [23] grafted various amine groups into pores of mesoporous silica materials, characterizing them as CO_2 adsorbents. Huang et al. [24] have reported CO_2 removal from natural gas by aminopropyl-functionalized MCM-48, and Chang et al. [25] have investigated CO_2 adsorption and desorption on aminopropyl-functionalized SBA-15.

Kim [26] reported that, at 298 K and PCO_2=1 atm, CO_2 adsorption capacity of attached amine to MCM-48 sample after 40 min was 0.8, 0.4, 0.3, and 0.1 m·mol/g for aminopropyl (APS) - polyethyleneimine (PEI) - pyrrolidinepropyl (pyrps) and polymerized aminopropyl (P-APS) -MCM-48, respectively. APS-MCM-48 displayed the highest CO_2 adsorption rate and capacity under these experimental conditions despite the relatively low concentration of surface amino groups. PEHA has more amine groups compared to tetraethylenepentamine (TEPA) and as a result is a better adsorbent for CO_2. Also, MCM-48 is more economical compared to SBA-15 since P_{123} is not used in its manufacture.

In this study, CO_2 adsorption on amine modified mesoporous silica MCM-48 was investigated. CO_2 adsorption capacity was measured by the volumetric method at 298 K up to 5 bar.

EXPERIMENTAL

1. Preparation of MCM-48 Silica

All materials were obtained from Merck. MCM-48 mesoporous silica was synthesized using cetyltrimethylammonium bromide (CTAB) as cationic surfactant and tetraethyl orthosilicate (TEOS) as the silica source. 10 ml of TEOS was mixed with 50 ml of deionized water and the mixture stirred for 1 h at 313 K. Then 0.9 g of NaOH and 0.19 g of KBr was added into the mixture and stirred for 1 h, after that 10.61 g of CTAB as the surfactant was added to the solution and stirred for 1 h. The mixture was transferred to an autoclave, and under static conditions the reaction was carried out at 433 K for 48 h. The resulting product was filtered and five times washed with distilled water and dried at 373 K. Finally, synthesized samples were calcined in the air for 4 h at 823 K, increasing the temperature to 823 K at 1 °C/min of the heating rate [27].

2. Preparation of Nanocomposite MCM-48-PEHA-DEA

Amine modified MCM-48 was prepared by use of impregnation and formation of hydrogen bonds between MCM-48 and amines (Fig. 1). The given amount of PEHA (P) and DEA (D) was dis-

†To whom correspondence should be addressed.
E-mail: anbia@iust.ac.ir

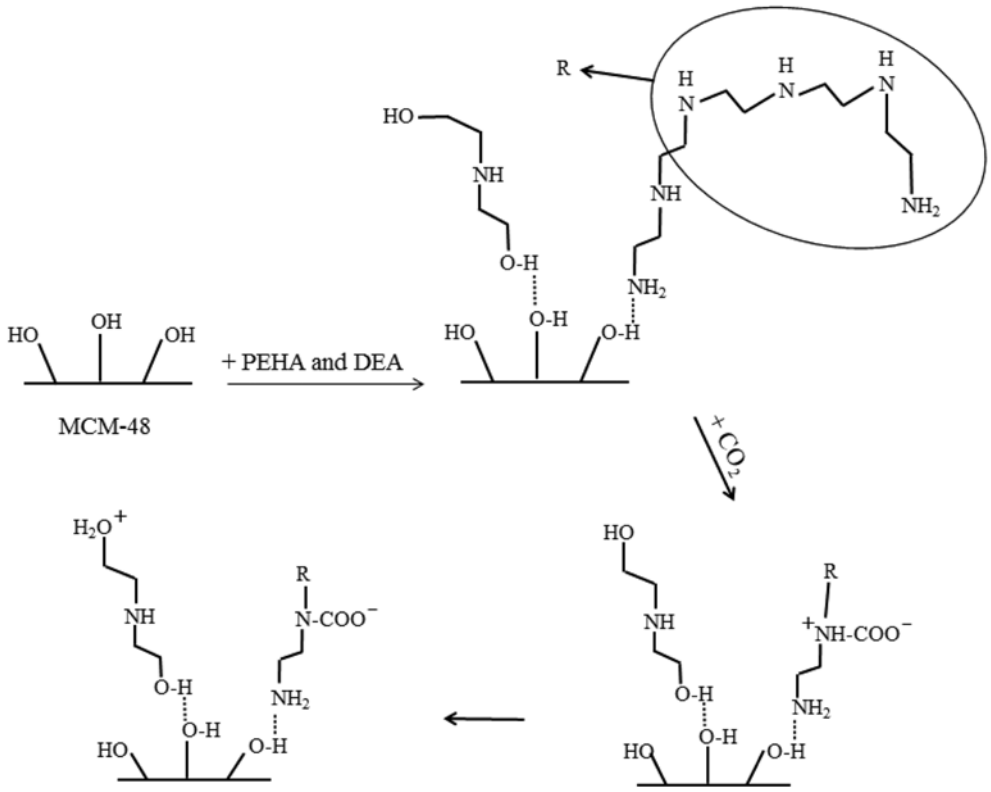

Fig. 1. Reaction of CO_2 with mixture of PEHA and DEA.

solved in 20 g of ethanol under stirring for 0.5 h, and then 0.4 g of calcined MCM-48 sample was added into the solution. The mixture was stirred and refluxed for 2 h at 353 K. The mixture was evaporated at 353 K followed by drying at 373 K for 1 h. In all samples, the weight percent of amines was fixed to 50 wt%. The weight percent of various amines was then determined by the added amine amounts in the preparation process. These adsorbents were denoted as MCM-48-mP-nD, where m and n represent the weight percentage of PEHA and DEA in the samples, respectively. For example, when MCM-48 was used as support and loaded with 50% mixed amines (35 wt% PEHA and 15 wt% DEA), the obtained sample was named as MCM-48-35P-15D, which contained 50 wt% MCM-48 support, 35 wt% PEHA and 15 wt% DEA. Quantities of added PEHA, DEA, MCM-48 and ethanol are given in Table 1.

3. Characterization of Adsorbents

MCM-48 as support and MCM-48-35P-15D as optimized adsorbent are characterized in this study. X-Ray diffraction spectrum was obtained on a Philips 1830 diffractometer using Cu-K_α radiation of wavelength 0.154 nm. XRD pattern was obtained between 1° and 10° with a scan speed of $1^0 \cdot min^{-1}$. Adsorption-desorption isotherms were measured at 77 K on a Micromeritics model ASAP 2020 sorptometer. The Brunauer-Emmet-Teller (BET) specific surface areas were calculated using adsorption data acquired at the relative pressure (P/P_0) range of 0.2-0.4 and the total pore volume determined from the amount adsorbed at the relative pressure of about 0.99. The pore size distribution curves of samples were calculated from the analysis of the adsorption branch of the isotherm using the Barrett-Joyner-Halenda (BJH) algorithm. FT-IR spectra of the adsorbents were recorded at room temperature on a DIGILAB FTS 7000 spectrometer equipped with an attenuated total reflection (ATR) cell.

Table 1. Amounts of PEHA, DEA, MCM-48 and ethanol used for the impregnation of MCM-48-PEHA-DEA sample

Sample name	Weight of MCM-48 (g)	Weight percent of PEHA	Weight percent of DEA	Weight of ethanol (g)
MCM-48-25P-25D	0.40	25	25	20
MCM-48-30P-20D	0.40	30	20	20
MCM-48-35P-15D	0.40	35	15	20

4. CO_2 Adsorption Measurement

To investigate the CO_2 adsorption capacity of samples, a standard system based on volumetric method was used that is schematically illustrated in Fig. 2. 1 g of sample was loaded inside the sample cell (13) and attached to the system. Then the system was carefully checked with the inert Helium gas flow to ensure all connections have no leakage. The existing gas inside the system was swept out with Helium. Afterwards, to remove residual solvents trapped in nanopores during synthesis, all the valves except 11, 10, 9 and 8 were closed and the system was vacuumed and heated at 473 K for 1.5 h. Ultra-high purity carbon dioxide (99.999%) was introduced into adsorption unit for the CO_2 adsorption measurements. To perform an adsorption test, the valve of the CO_2 cylinder was opened and the CO_2 pressure was regulated at the desired value, then valves 7 and 8 were opened to reach a pressure balance in the reference cell (12). Afterwards, valve 10 was immediately opened and the pressure decrease was recorded. The pressure of adsorption cell decreased due to some dead volume and some CO_2 adsorption.

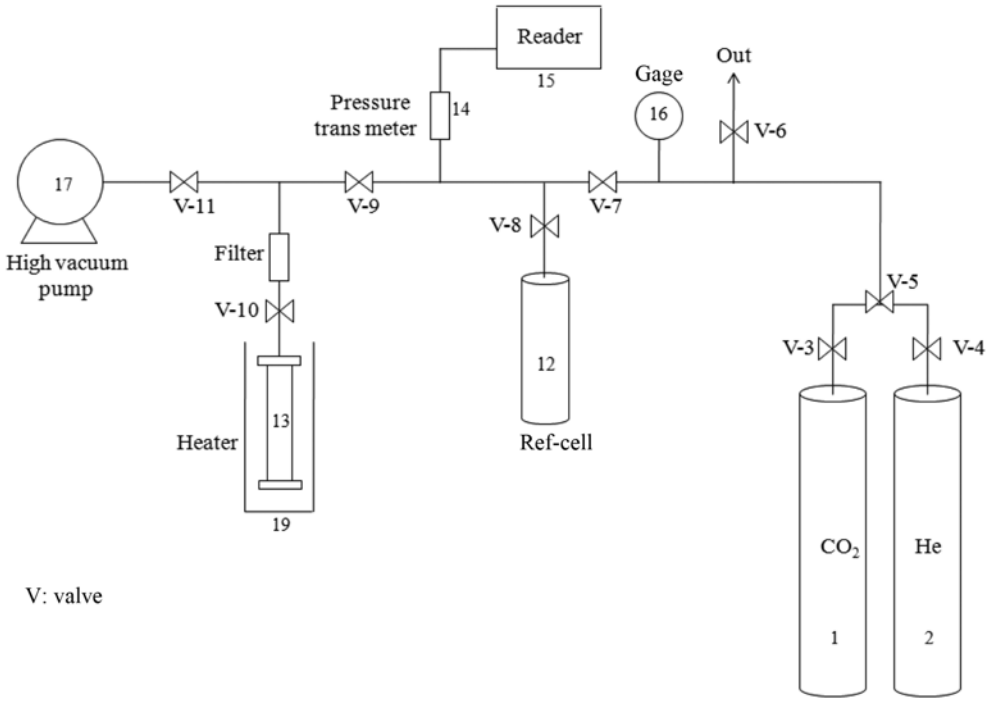

Fig. 2. Schematic diagram of volumetric set up for adsorption test.

The portion of dead volume was calculated via helium tests and subtracted from the total pressure change. Finally, the exact pressure decrease resulting from CO_2 adsorption could be calculated.

RESULTS AND DISCUSSION

1. XRD Analysis

The powder X-Ray diffraction patterns (XRD) of MCM-48 silica before and after amine attachment are shown in Fig. 3. The XRD patterns of calcined mesoporous MCM-48 powders (a) exhibited two peaks at 2θ smaller than 3^0 and a series of weak peaks in range $3.5\text{-}5.5^0$ as expected for a MCM-48 phase. They are assigned to the (211), (220), (420), and (422) reflections, which can be indexed to Ia3d cubic structure, are clearly observed [28]. The XRD patterns of MCM-48 did not change significantly after PEHA and DEA attachment (B). However, the peak intensity decreased slightly. The peak intensity is a function of the scattering contrast between the MCM-48 walls and pore channels and decreases with decreasing scattering contrast after attachment of amino groups to the pore surface [29]. Hence, the observed decrease of the XRD peak intensity is probably due to the pore filling by amine groups [30,31].

2. FT-IR Analysis

The FT-IR spectra of MCM-48 and Amine-attached MCM-48 samples are shown in Fig. 4. In the spectra of MCM-48 (A), a broad adsorption bond at around 3,500 cm^{-1} is assigned to O-H stretch-

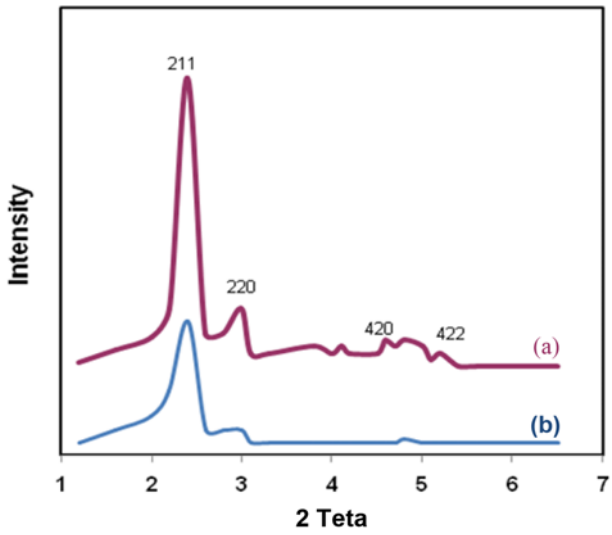

Fig. 3. XRD patterns of the MCM-48 (a) and MCM-48-35P-15D (b).

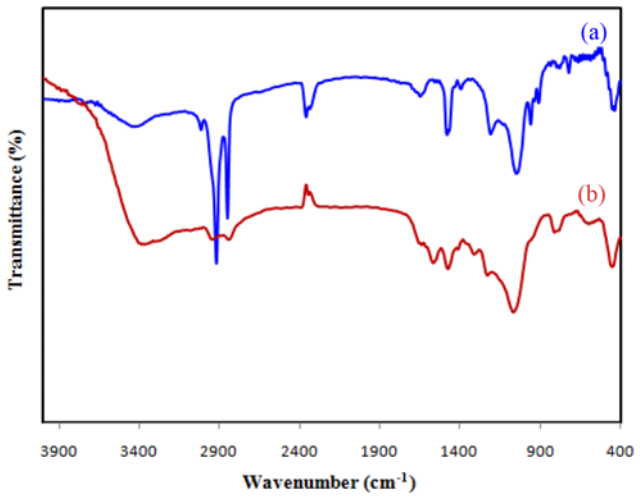

Fig. 4. FT-IR spectra of MCM-48 (a) and amine modified MCM-48 (b).

ing bonds of silanol group [32]. Si-O band stretching was detected at 976 cm^{-1}. The FT-IR spectra of MCM-48-35P-15D showed a broad NH_2 stretching at 3,250-3,450 cm^{-1}. The bonds in the region of 1,510 and 1,590 cm^{-1} are due to asymmetric and symmetric bending of the primary amine groups. A broad adsorption band at 3,400 cm^{-1} is assigned to O-H stretching bonds of DEA and confirms that the MCM-48 has been functionalized.

3. N_2 Adsorption-desorption Isotherms Analysis

Fig. 5(a) and (b) illustrate nitrogen adsorption isotherms and pore size distributions of MCM-48 (A) and MCM-48-35P-15D (B), respectively. From Fig. 4(a), it can be seen that calcined MCM-48 materials exhibit typical type IV isotherms. For mesoporous molecules, the sharpness and height of the capillary condensation step in the isotherms indicate the pore size uniformity [33]. Table 2 shows the pore size, BET surface area and total pore volume of these samples. Calcined MCM-48 showed BET surface area of about 1,312 m^2/g and pore volume of 1.22 cm^3/g. After loading of 50 wt% amines (PEHA and DEA), the adsorbed volume of nitrogen decreases distinctly. This phenomenon suggests the occupation of the pores by the amines. As shown in Table 2, the BET surface area and pore volume of MCM-48-35P-15D decreased to 572 m^2/g and 0.41 cm^3/g, respectively, which also confirms that amines have occupied the channel of MCM-48.

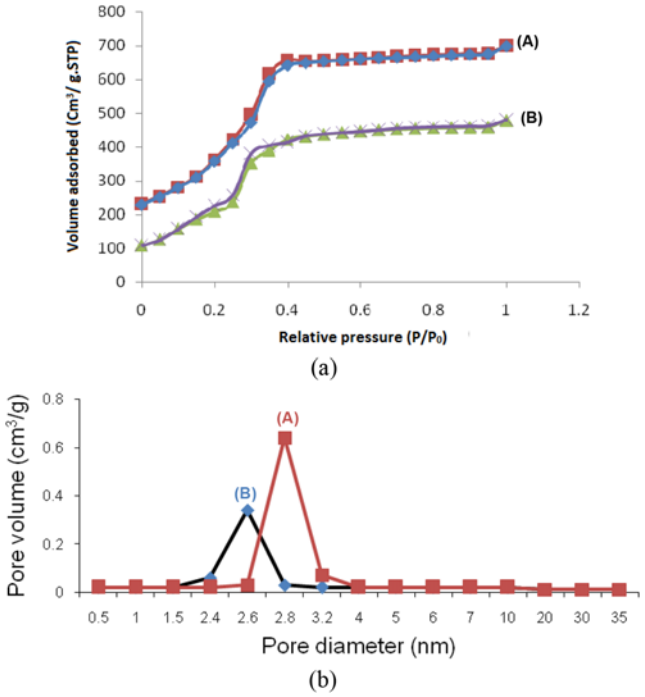

Fig. 5. (a) The N_2 adsorption-desorption isotherms of MCM-48 (A) and MCM-48-35P-15D (B) powders at 77 K. (b) Pore size distributions of MCM-48 (A) and MCM-48-35P-15D (B).

Table 2. Textural properties of calcined MCM-48 and MCM-48-35P-15D

Sample	S_{BET} (m^2/g)	Pore diameter (Å)	Pore volume (cm^3/g)
Calcined MCM-48	1312	3.1	1.22
MCM-48-35P-15D	572	2.6	0.41

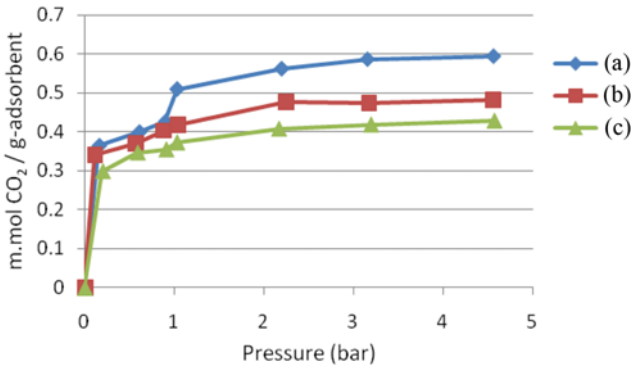

Fig. 6. CO_2 adsorption capacity at 298 K, MCM-48-35P-15D (a), MCM-48-30P-20D (b), MCM-48-25P-25D (c).

4. Isotherms of CO_2 Adsorption

Fig. 6, displays the CO_2 adsorption capacity of amine modified MCM-48 at room temperature (298 K) and different pressures in the range 0-5 bar. At pressure 1 bar and 298 K, MCM-48-35P-15D shows the highest CO_2 adsorption capacity of 0.51 m·mol/g. Under these conditions, MCM-48-25P-25D and MCM-48-30P-20D show CO_2 adsorption capacity of 0.36 m·mol/g and 0.42 m·mol/g, respectively, while conditions MCM-48-PEHA-50 (50 is weight percent of loaded PEHA), show CO_2 adsorption capacity of 0.26 m·mol/g. Increasing the pressure from 0.16 bar to 4.57 bar, the CO_2 adsorption capacity of MCM-48-35P-15D, is shifted from 0.36 m·mol/g to 0.59 m·mol/g.

Fig. 7 shows the changes of CO_2 adsorption capacity with the increase of PEHA percentage in loaded amines. Since the density of amine groups increases with the increase in weight percent of PEHA, CO_2 adsorption capacity is enhanced and reached from 0.36 to 0.51 (m·mol/g) when 25 wt% PEHA increased to 35 wt%.

In Table 3, features of different CO_2 adsorbents are recovered. The hydroxyl groups change the chemical adsorption mechanism. Without the presence of hydroxyl group, the main reaction to account for CO_2 removal is as follows:

(1) $CO_2+2\ R_2NH=R_2NH_2^+ + R_2NCOO^-$.

In the presence of hydroxyl group, the formation of carbamate type

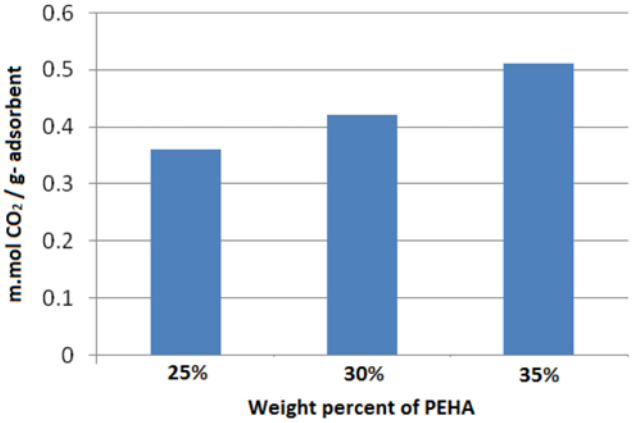

Fig. 7. Influence of the amount of PEHA loading on CO_2 adsorption capacity (PCO_2=1 atm).

Table 3. Comparison of different CO_2 adsorbents

Adsorbent	CO_2 pressure (bar)	Temperature (K)	CO_2 adsorption capacity (m·mol/g)	Reference
MCM-48-APS	1	298	~0.65	[34]
MCM-48-Pyrps	1	298	~0.08	[34]
MCM-48-P-APS	1	298	~0.03	[34]
MCM-48-PEI	1	298	~0.3	[34]
MCM-48- Cl-PEI	1	298	0.4	[37]
MCM-48- Cl-Pyr	1	298	0.3	[37]
SP-DEA	-	-	0.47	[36]
SC-DEA	-	-	0.2	[36]
SP-30T-20D	-	-	3.7	[36]
PEI-MCM-48	-	-	2.7	[38]
MCM-48-35P-15D	1	298	0.51	[This study]

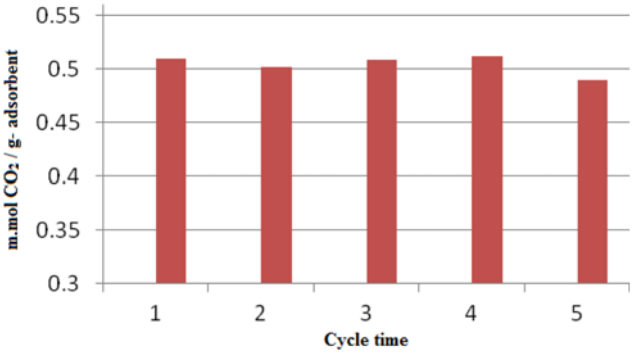

Fig. 8. Cycle adsorption of CO_2 by MCM-48-35P-15D sample.

zwitterions may be promoted as following reaction [34,35],

(2) $CO_2+ROH+R_2NH=ROH_2^+ +R_2NCOO^-$.

Usually each mole of amine reacts with 0.5 mole of CO_2 to form carbamate. However, the existence of a hydroxyl group changes the mechanism and the carbamate further reacts with CO_2 to form bicarbamate or carbamate type zwitterions [30,31]; therefore, one mole of amine reacts with one mole of CO_2 and thus the adsorption capacity is enhanced [36].

According to Kim's report [26], after 5 min at 298 K and PCO_2= 1 atm, CO_2 adsorption capacity was 0.03, 0.08 and 0.3 m·mol/g, P-APS-MCM-48, Pyrps-MCM-48 and PEI-MCM-48, respectively, whereas in these conditions, MCM-48-35P-15D displayed CO_2 adsorption capacity of 0.51 m·mol/g, much higher than P-APS- MCM-48 and Pyrps-MCM-48, and about 1.5 times of PEI-MCM-48.

Fig. 8 depicts the adsorptive behavior of MCM-48-35P-15D sample in the cyclical adsorption of CO_2 performed using the pure CO_2 at 298 K and 1 bar. The adsorbed CO_2 was desorbed by increasing the temperature to 473 K, the system was then cooled to 298 K and the CO_2 adsorption of the same compound was measured again. This adsorbent exhibits a high stable adsorption capacity of pure CO_2. Its adsorptive capacity in the 5th cycle with pure CO_2 is 0.49 m·mol/g, only slightly lower than that in the 1st cycle (0.51 m·mol/g), which is important for the potential application of this CO_2 adsorbent.

CONCLUSIONS

CO_2 adsorption on nanocomposite containing MCM-48 modified by the mixture of Pentaethylenehaxamine (PEHA) and diethanolamine (DEA) was investigated. MCM-48-35P-15D showed the highest CO_2 adsorption capacity of 0.51 m·mol/g at temperature of 298 K and PCO_2=1 atm, whereas, in these conditions MCM-48-PEHA-50 showed CO_2 adsorption capacity of 0.26 m·mol/g. By increasing the pressure from 0.16 bar to 4.57 bar, CO_2 adsorption capacity of MCM-48-35P-15D shifted from 0.36 m·mol/g to 0.59 m·mol/g. Presence of hydroxyl group (DEA) can enhance adsorption of CO_2 on attached amine to MCM-48. As each molar amine group can capture two molars of CO_2, the formation of carbamate type zwitterions, the hydroxyl group can enhance CO_2 adsorption capacity. The CO_2 adsorption capacity of the mixture amine modified MCM-48 sample reaches 0.51 m·mol/g at 298 K and PCO_2= 1 atm, that is larger than P-APS, PEI and Pyrps grafted to MCM-48 and other adsorbents.

REFERENCES

1. Intergovernmental Panel on Climate Change (IPCC), Climate Change 1995: *The Science of Climate Change*, Cambridge University Press (1996).
2. E. Bryant, *Climate Process and Change*, Cambridge University Press, Cambridge, UK (1997).
3. T. Yokoyama, *In Separations Technology*, Queensland, Australia (2006).
4. D. Aaron and C. Tsouris, *Sep. Sci. Technol*., **40**, 321 (2005).
5. E. S. Kikkinides, R. T. Yang and S. H. Cho, *Ind. Eng. Chem. Res*., **32**, 2714 (1993).
6. S. H. Hyun, J. K. Song, B. I. Kwak, J. H. Kim and S. A. Hong, *J. Mater. Sci*., **34**, 309 (1999).
7. P. J. E. Harlick and A. Sayari, *Ind. Eng. Chem. Res*., **46**, 446 (2007).
8. R. J. Hook, *Ind. Eng. Chem. Res*., **36**, 1779 (1997).
9. C. S. Tan and J. E. Chen, *Sep. Purif. Technol*., **49**, 174 (2006).
10. H. M. Krutka, S. J. Sjostrom and C. J. Bustard, *Paper #08-A--Mega-AWMA*., **173** (2008).
11. K. T. Chue, J. N. Kim, Y. J. Yoo, S. H. Cho and R. T. Yang, *Ind. Eng. Chem. Res*., **34**, 591 (1995).
12. M. Katoh, T. Yoshikawa, T. Tomonari, K. Katayama and T. Tomida, *J. Colloid Interface Sci*., **226**, 145 (2000).
13. T. Mimura, H. Simayoshi, T. Suda, M. Iijima and S. Mituoka, *Energy Convers. Manage., Suppl*. S., **57**, 38 (1997).
14. C. L. Leci, *Energy Convers. Manage., Suppl*. S., **57**, 38 (1997).

15. J. E. Critchfield, W. Y. Su, T. J. Kenney and P. E. Holub, US Patent, 5,861,051 (1996).
16. M. Anbia and S. A. Hariri, *Desalination*, **261**, 61 (2010).
17. M. Anbia and M. Lashgari, *Chem. Eng. J*., **150**, 555 (2009).
18. M. Anbia and S. E. Moradi, *Appl. Surf. Sci*., **255**, 5041 (2009).
19. M. Anbia and S. E. Moradi, *Chem. Eng. J*., **148**, 452 (2009).
20. M. Anbia, N. Mohammadi and K. Mohammadi, *J. Hazard. Mater*., **176**, 965 (2010).
21. S. C. Shen, X. Chen and S. Kawi, *Langmuir*., **20**, 9130 (2004).
22. A. Macario, A. Katovic, G. Giordano, F. Iucolano and D. Caputo, *Micropor. Mesopor. Mater*., **81**, 139 (2005).
23. A. L. Chaffee, S. W. Delaney and G. Knowles, *Abstr. Pap. 223rd ACS Nat*., Meeting P (2002).
24. H. Y. Huang, R. T. Yang, D. Chinn and C. L. Munson, *Ind. Eng. Chem. Res*., **42**, 2427 (2003).
25. A. C. C. Chang, S. S. C. Chuang, M. Gray and Y. Soong, *Energy Fuels*, **17**, 468 (2003).
26. S. Kim, J. Ida, V. V. Guliants and Y. S. Lin, *J. Phys. Chem*., B **109**, 6287 (2005).
27. M. Anbia and N. Mohammadi, *J. Porous. Mater*., **18**, 13 (2011).
28. V. Alfredsson and M. W. Anderson, *Chem. Mater*., **8**, 1141 (1996).
29. L. Mercier and T. Pinnavaia, *J. Environ. Sci. Technol*., **32**, 2749 (1998).
30. H. Yoshitake, T. Yokoi and T. Tatsumi, *Chem. Mater*., **14**, 4603 (2002).
31. X. Xu, C. Song, J. M. Anderson, G. B. Miller and A. W. Scaroni, *Energy Fuels*, **16**, 1463 (2002).
32. C. P. Jaroniec, M. Kruk, M. Jaroniec and A. Sayari, *J. Phys. Chem*., B, **102**, 5503 (1998).
33. R. A. Pierotti, J. Rouquerol and T. Siemieniewska, *J. Pure Appl. Chem*., **57**, 603 (1985).
34. O. Leal, C. Bolivar, C. Ovalles, J. J. Garcia and Y. Espidel, *Inorg. Chim. Acta*, **240**, 183 (1995).
35. S. Satyapal, T. Filburn and J. Trela, *Energy Fuels*, **15**, 250 (2001).
36. M. B. Yue, L. B. Sun, Y. Cao, Z. J. Wang, Y. Wang, Q. Yu and J. H. Zhu, *Micropor. Mesopor. Mater*., **114**, 74 (2008).
37. S. Kim, J. Ida, V. V. Guliants and J. Y. S. Lin, *J. Phys. Chem. B*., **109**, 6287 (2005).
38. W. J. Son, G. S. Choi and W. S. Ahn, *Micropor. Mesopor. Mater*., **113**, 31 (2008).